The Formation and Structure of Suspension-Polymerized Styrene–Divinylbenzene Copolymers

G. J. HOWARD and C. A. MIDGLEY,* *Department of Polymer and Fibre Science, University of Manchester Institute of Science & Technology, Manchester, England*

Synopsis

Porous polymers were prepared by suspension copolymerization of styrene/divinylbenzene in various ratios together with various quantities of diluents, both solvating and nonsolvating. Parallel bulk polymerizations were made to detect the onset of gelation and phase separation. The dry polymeric beads were examined by a range of techniques: apparent densities; mercury porosimetry; nitrogen sorption/desorption isotherms, vapor sorption, equilibrium swelling, and electron microscopy. The properties of the porous polymers are discussed in terms of phase separation during polymerization consequent on either an unfavorable polymer–solvent interaction or a microsynaeresis.

INTRODUCTION

The development of internally porous polymer particles has been of considerable significance in ion exchange[1] and gel permeation[2] chromatography. These porous materials are also of potential interest as carbon precursors[3] and as the matrix for polymer-bound reagents. There is a need to establish both the mechanism by which the pores are generated and the relationship between the conditions of polymerization and the properties of the resultant polymer. The present report is intended as a contribution to these objectives.

EXPERIMENTAL

Larger-scale preparations of porous, crosslinked polystyrene particles were by a method similar to that of Millar et al.[4] Polymerization was carried out at 80°C. A single batch of divinylbenzene (Koch-Light Laboratories) was used throughout; the composition is as in Table I.

Inhibitor was removed by extracting three times with 2*M* sodium hydroxide followed by three water washes, the identical procedure being followed for the styrene (Fisons). The initiator (azoisobutyronitrile, recrystallized from methanol) was dissolved in the selected monomer mixture at 0.4% (w/v), and this (a volume between 180 and 450 cm^3, depending on composition) was then added to 1 L 1% aqueous solution of Promulsin (Watford Chemical Co.) at 80°C with vigorous agitation. After dispersion, the stirrer was set to a lower level and the reaction allowed to proceed for 24 h. Then, a 2% solution of *t*-butylcatechol in toluene was added, and after a further hour, the reaction vessel was removed from the thermostat and the polymer beads filtered off through fine stainless steel mesh (nominal aperture size 0.075 mm). After thorough washing with water,

*Present address: Polysar France, La Wantzenau, France.

Journal of Applied Polymer Science, Vol. 26, 3845–3870 (1981)
 CCC 0021-8995/81/113845-26$02.60

TABLE I
Composition (vol %) of Divinylbenzene Sample

Divinylbenzene (mixed *o*- and *p*- isomers)	55.7%
Ethylstyrene	37.3%
Diethylbenzene	3.5%
Other saturated compounds	3.5%

the beads were transferred to a large volume of 2*M* hydrochloric acid and boiled for 10 min to hydrolyze any remaining cellulosic suspension stabilizer. The product was the filtered through glass fiber filter paper, washed free of acid with water, and then repeatedly washed with acetone and finally dried in vacuo at 80°C. Yields were essentially quantitative to give spherical beads of 0.1 to 0.5 mm in diameter.

The coding of samples is as follows. The first number is the volume fraction of divinylbenzene isomers in the mixed monomers; the second number is the volume fraction of diluent (including the inert compound from commercial divinylbenzene) in the organic phase, while the final letter identifies the diluent.

Because visual assessment of phase separation within beads during polymerization cannot easily be made and recovery of low-conversion samples is difficult, a series of bulk polymerizations were also made at the same monomer and diluent compositions as used in the suspension copolymerization. Tubes of 6 mm internal diameter and about 500 mm long were used; these were pretreated internally with dimethyldichlorosilane to ease subsequent removal of polymer. About 10 cm^3 reaction medium was added and several freeze–thaw cycles made before sealing the frozen contents in vacuo. Approximate calculation shows that the heat of polymerization can be dissipated through the vessel walls with a temperature differential of ca. 1°C between contents and thermostat bath. The visual appearance of the reaction medium was followed for 36 min, and the experiment was repeated twice.

The following procedure was employed to determine the conversion to polymer and to gel. Samples of a given reaction composition were sealed into several tubes which were placed together into the bath at 80°C. Tubes were removed one at a time and immediately quenched in ice water. After cooling, the dried tubes were opened at both ends and quickly weighed. A portion (ca. 3 g) of the reaction mixture was forced from the tube with a closely fitting preweighed rod into a solution of *t*-butylcatechol in methanol. The tube and rod were reweighed and a second portion forced into toluene, also containing *t*-butyl catechol. The mass of this second portion was also found by difference. After crushing, the portions of reaction mixture were allowed to stand under the appropriate liquid for 24 h, after which time they were poured into prepurified Soxhlet thimbles and stood in a further volume of extracting liquid for 24 h before being Soxhlet extracted for a further day. Finally, the thimbles and contents were dried in vacuo at 80°C, the swollen product from the toluene extraction being first Soxhleted in methanol to speed the drying process. The weights of insoluble material was converted to fractional conversions to polymer (methanol insoluble) and to gel (toluene insoluble).

The density of polymer beads was found by pyknometry with mercury as confining fluid. The beads were outgassed in the pyknometer before it was filled

under vacuum with mercury. After thermal equilibration for 30 min at 25°C, the mercury in the stem was drawn off to a fixed level using a square-cut hypodermic needle inserted to its full length into the capillary.

Mercury intrusion porosimetry measurements were made with an Amino-Winslow porosimeter, and we are indebted to Dr. G. R. Heal of the University of Salford for making this instrument available to us. Cumulative pore volumes were calculated by standard techniques,[5] and pore radii quoted are those of the equivalent hollow cylinders.

Nitrogen adsorption at −196°C was determined volumetrically in an apparatus constructed along the lines of that proposed by Crowl,[6] and the procedure of the British Standards manual[7] was followed. The BET equation[8] was used to analyze the low relative pressure region of the isotherm in order to find the surface areas of the beads. For those samples for which desorption from high relative pressure (ca. 0.985) was measured, the data were treated by application of the Kelvin equation as described in detail by Gregg and Sing.[9] To check the operation of the apparatus, the surface area of a graphitized carbon was found and the measurement repeated after an interval of one year. The same value of 82.2 m^2/g was obtained in good agreement with the value at 81.5 m^2/g determined independently on the same sample in another laboratory. The N.P.L. standard mesoporous silica (surface area 286.2 ± 3.5 m^2/g) was also measured and gave a result of 282.1 m^2/g. A crosslinked polystyrene bead sample from among those prepared in this work was measured on three separate occasions to give surface areas of 425.2, 432.6, and 446.3 m^2/g, which correspond to a coefficient of variation typical of this technique.[6]

The sorption of methanol and benzene vapors at 30 ± 0.1°C was found by a gravimetric technique. A McBain–Bakr[10] balance was constructed in which the extension of quartz springs carrying the samples was measured at various relative pressures. The apparatus was so designed as to be grease free, all gaskets and valve diaphragms being made of Viton A rubber. The whole apparatus was enclosed in an air thermostat. The quartz springs had a sensitivity of ca. 25 cm/g and were precalibrated in the apparatus, their extension being measured on a cathetometer reading to 0.01 mm.

The swelling of polymer beads in liquid toluene was measured by a method due to Pepper.[11] Cylinders, approximately 20 mm in diameter and 50 mm long and closed at one end, were made of wire mesh (nominal aperture size 0.075 mm). A sample (ca. 1.5 g), previously sieved through a mesh of 0.4 mm aperture, was placed into the mesh container and thoroughly flushed with water to remove any remaining fines before drying in vacuo at 80°C. The dried tube and sample were weighed and then placed in toluene and after a certain time were transferred to a glass centrifuge tube with a conical bottom. The centrifuge tube was sealed with a rubber cap and the contents centrifuged at 500 g for 45 min. After this, the mesh containing the swollen sample was weighed in a stoppered container before being replaced in toluene. This procedure was repeated until constant weight was reached. The time required for equilibrium swelling varied enormously with the bead structure. Beads polymerized in the absence of diluent and at low crosslinker content required up to 11 days for equilibration, whereas very porous beads swelled completely in a few hours. Some portions from the bulk polymerizations were also used in swelling experiments. However, these polymers, initially of diameter ca. 6 mm and length 50 to 100 mm, had not reached

equilibrium swelling in toluene after two months, and this method was then terminated.

The swelling of individual beads was also followed microscopically.[12] A single bead was swollen in a small sample tube filled with toluene and transferred occasionally to a toluene-filled cell on the microscope stage. Diameters were measured (magnification ×50) at right angles on the beads which had been selected for their sphericity. Ingress of toluene into a dry bead was readily visible, but the polymer continued to swell well after a uniformly transparent appearance had been reached. Results were recorded as the swelling ratio S, equal to $(D/D_0)^3$, where D is the diameter of the swollen bead, and D_0 is that of the original bead.

For transmission electron microscopy, individual beads were placed in 2.5% aqueous agar and, after it had gelled, were removed so as to retain a light coating of gel. They were then embedded in a polymeric resin which was found not to swell or deform the coated beads. Slices about 600 Å thick were cut on an ultramicrotome (LKB 4800 A) with a glass knife, mounted on Formvar-coated grids and examined in the electron microscope (AEI EM6B). Samples for scanning electron microscopy (Cambridge Stereoscan MK1) were mounted on metal stubs with adhesive and vacuum-coated with silver.

RESULTS

The polymers prepared for this investigation were designed to provide a crosssection of properties such as had been indicated by earlier work.[4,13] Series of copolymers were made at various diluent contents and approximately constant crosslinker and vice versa, using toluene and decane as representative solvating and nonsolvating diluents, respectively. Limited work with other diluents was mostly at a fixed diluent and crosslinker level. Table II lists the preparations reported and their visual appearance, which is related to the reaction composition.

TABLE II
Suspension-polymerized Copolymers and Their Visual Appearance (Dry)

Sample code	Appearance	Sample code	Appearance	Sample code	Appearance
.092/.385/T[a]	C[b]	.104/.408/D	T/0[c]	.104/.012[d]	C
.213/.415/T	C	.213/.415/D	O[d]	.213/.025	C
.322/.423/T	T[b]	.322/.423/D	O	.322/.037	C
.364/.410/T	T	.435/.432/D	O	.435/.051	C
.435/.432/T	T	.515/.250/D	O	.552/.063	C
.515/.420/T	T	.552/.439/D	O		
.555/.439/T	O[c]	.322/.231/D	T	.322/.423/XY[a]	T
.600/.430/T	O	.322/.616/D	O	.322/.423/BP[a]	O
.322/.231/T	C			.515/.420/BP	O
.322/.615/T	T			.322/.423/CE[a]	T
.322/.808/T	T			.322/.423/EB[a]	T

[a] T = Toluene, D = decane, XY = xylene, BP = dibutyl phthalate, CE = tetrachloroethane, EB = ethylbenzene.

[b] C = Clear, T = translucent, O = opaque.

[c] See text.

[d] No added diluent; second number refers to inert component from commercial divinylbenzene.

In two cases (see Table II), the product was not entirely homogeneous in appearance. With the toluene-modified sample (.555/.439/T), where all beads are white and opaque, a small proportion, which seemed to be larger than average, appeared noticeably whiter. Nonuniformity was more evident in the decane-modified beads (.104/.408/D). Here, about half the beads seemed totally opaque and half semitranslucent; a count on 100 beads gave 44 opaque and 56 translucent. A repeat polymerization was made with the same result. The two types of beads could not be separated by flotation. A close inspection of individual beads indicated slight differences within both groups, and it seems likely that a continuous gradation in structure exists which at a critical level produces a more discontinuous change in optical appearance. Certainly, the differentiation between beads is less obvious when viewed in blue light.

Bead polymers could not be produced by suspension polymerization beyond certain limits. With solvating diluents, the practical limit at high diluent contents is largely one of polymer yield; but with nonsolvating diluents, there is a more clearly defined upper bound. At crosslinker volume fractions ca. 0.3, powders rather than beads are formed above 0.6 volume fraction decane; while at 0.5 volume fraction crosslinker, beads could not be made at 0.4 diluent volume fraction. Further, the experimental technique used did not permit the production of diluent-modified homopolystyrene beads because of agglomeration in the working-up stages.

As mentioned in the experimental section, a knowledge of the progress of reaction is obtained from small-scale homogeneous polymerizations. The conversion to polymer, as judged by the relative amount of methanol-insoluble material, is shown in Figure 1 as a function of time for reactions with a (nearly) constant volume of toluene (solvating) diluent but varying proportions of divinylbenzene isomers. In all cases, there is an initial acceleration which is considered to be an intrinsic feature of the reaction since temperature equilibration is reached some 30 s after introduction of the reaction tube into the bath. A degree of autoacceleration, a consequence on diffusion-controlled chain termination, may be occurring in the viscous reaction medium. Evidence has been reported for autoacceleration in the homopolymerization of styrene.[14,15] The increased rate of polymerization at higher crosslinker contents may be a consequence of autoacceleration, but two other factors need to be considered. First, there is the higher reactivity of the double bonds in divinylbenzene, especially those of the paraisomer; and, secondly, since some unreacted double bonds from crosslinker molecules will be trapped in the methanol-insoluble polymer, the fractional conversion to polymer at any stage will exceed the corresponding consumption of double bonds.

Precisely analogous features are evidenced (Fig. 2) at approximately 0.4 volume fraction of decane (nonsolvating diluent) and a range of divinylbenzene contents. The initial rates of polymerization are slightly greater with decane as diluent (Table III). The earlier precipitation during polymerization in the presence of decane will effectively increase reactant concentrations, may enhance autoacceleration, and favor the entrapment of unreacted double bonds.

At a fixed monomer composition (0.322 volume fraction divinylbenzene), the polymerization rate depends on diluent content (Figs. 3 and 4), thus indicating an apparent order in monomer greater than unity; again, the decane-modified systems react faster (Table IV).

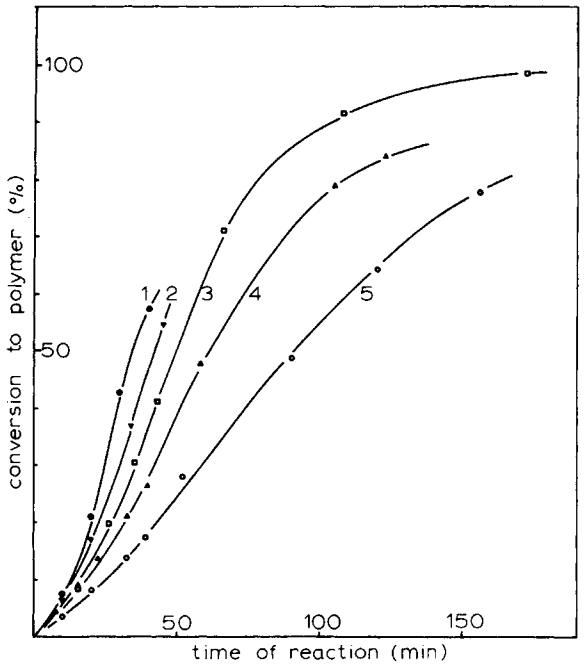

Fig. 1. Conversion to polymer as function of time for toluene-modified samples: Curve 1, .552/.439/T; Curve 2, .435/.432/T; Curve 3, .322/.423.T; Curve 4, .213/.415/T; Curve 5, .092/.385/T.

TABLE III
Initial Rates of Polymer Formation at Different Crosslinker Contents

Approx. 0.4 volume fraction tolune		Approx. 0.4 volume fraction decane	
Volume fraction divinylbenzene in monomers	Fractional conversion in 30 min reaction	Volume fraction divinylbenzene in monomers	Fractional conversion in 30 min reaction
0.092	0.126	0.104	0.141
0.213	0.190	0.213	0.240
0.322	0.242	0.322	0.315
0.435	0.308	0.435	0.387
0.552	0.430	0.552	0.457

Whereas polymer conversion is measured by the methanol-insoluble content, conversion to gel is estimated from the fraction of toluene-insoluble material since this liquid will dissolve the nongel polymer species. In all reactions, gelation occurs at an early stage, and only those samples taken very soon after commencement of polymerization are gel free. The polymer and gel contents rapidly converge, and no sol polymer is detectable beyond ca. 30% conversion. Extrapolation of the gel conversion curves to zero gel content gives a gel time from which the fractional conversion at gelation may be found (Table V). It must be appreciated, however, that these estimates are inevitably of low accuracy.

The gel point, as expected, occurs earlier in reaction as the crosslinker content is increased. At lower crosslinker contents, the decane-modified systems gel at lower conversions, and gelation is always more rapid in the absence of diluent.

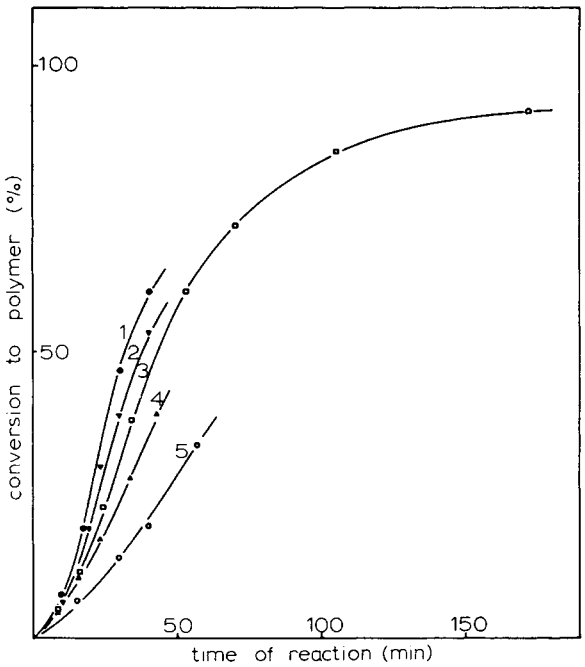

Fig. 2. Conversion to polymer as function of time for decane-modified samples: Curve 1, .552/.439/D; Curve 2, .435/.432/D; Curve 3, .322/.423/D; Curve 4, .213/.415/D; Curve 5, .104/.408/D.

At a fixed crosslinker content (0.32 volume fraction), the conversion at gelation is not sensitive to monomer concentration.

The gel time was also measured by repeating several of the reactions at a larger

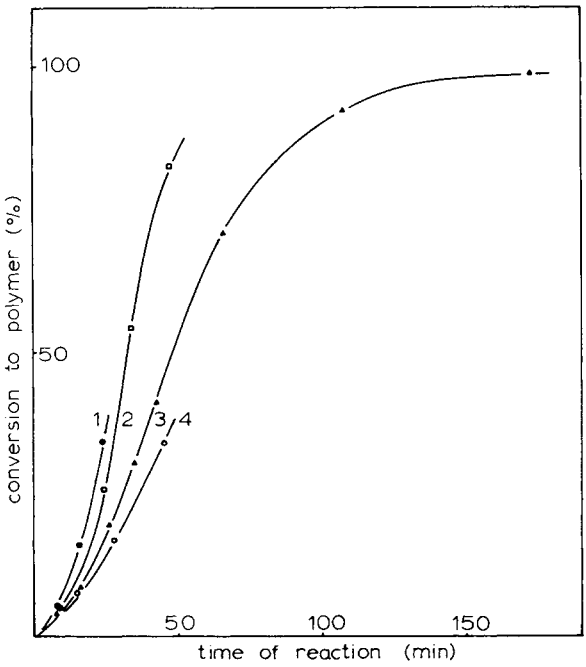

Fig. 3. Conversion to polymer as function for time for toluene-modified samples: Curve 1, .322/.037; Curve 2, .322/.231/T; Curve 3, .322/.423/T; Curve 4, .322/.615/T.

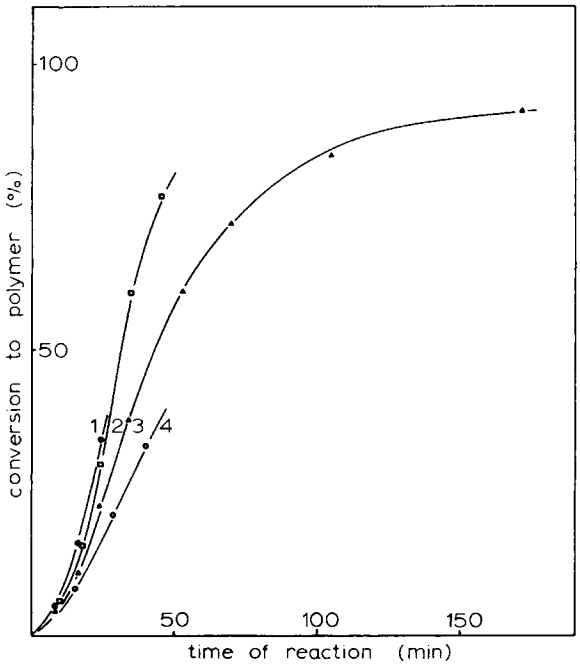

Fig. 4. Conversion to polymer as function of time for decane-modified samples: Curve 1, .322/0.37; Curve 2, .322/.231/D; Curve 3, .322/.423/D; Curve 4, .322/.616/D.

quantity (×2.5) in a conical flask fitted with a T-shaped stirrer. The gel time was taken as the point at which the reaction mixture "climbed up" the stirrer or, at higher crosslinker contents, suddenly broke into pieces. These gel times were repeatable to ±15 s and are corrected by deduction of half the time required for the reaction to reach equilibrium temperature. The values listed in Table V are always significantly greater than those based on the appearance of toluene-insoluble polymer. The most likely explanation of this observed discrepancy (which is well outside the experimental uncertainty) is that gelled polymer is formed initially as a microgel and gross elastic effects are shown only when these regions join up into a continuous phase. Similar observations have been reported by Bobalek et al.[16] for alkyd resins and by Storey[17] for styrene/divinylbenzene copolymers.

The occurrence of phase separation is clearly of critical importance in any discussion of the effect of solvation strength of the diluent on final polymer morphology. The cloudiness of the reactions carried out in thin tubes was judged

TABLE IV
Initial Rates of Polymer Formation at Different Dilutent Contents

0.322 volume fraction divinylbenzene in monomers			
Volume fraction toluene	Fractional conversion in 30 min	Volume fraction decane	Fractional conversion in 30 min
0.037[a]	0.500	0.037[a]	0.500
0.231	0.425	0.231	0.475
0.423	0.235	0.423	0.310
0.615	0.189	0.615	0.229

[a] Inert component from commercial divinylbenzene.

TABLE V
Time of Reaction and Conversion at Gel Point

Volume fraction divinyl-benzene in monomer	Toluene				Decane				No diluent		
	Volume fraction diluent	t_g[a]	f_g[b]	t_g^*[c]	Volume fraction diluent	t_g	f_g	t_g^*	t_g	f_g	t_g^*
0.10	0.42	17.2	0.068	24.3	0.42	12.5	0.055	22.3	9.5	0.045	10.3
0.21	0.42	10.0	0.052	15.3	0.42	7.5	0.040	15.5	5.5	0.030	6.0
0.32	0.42	7.5	0.038	11.8	0.42	8.0	0.038	12.0	4.0	0.026	4.8
0.44	0.42	6.0	0.032	10.3	0.42	6.5	0.032	9.8	2.5	0.017	—
0.55	0.42	5.5	0.030	—	0.42	5.5	0.030	—	2.0	0.012	—
0.32	0.23	7.0	0.042	—	0.23	7.0	0.038	—	—	—	—
0.32	0.62	7.0	0.042	—	0.62	9.5	0.040	—	—	—	—

[a] Gel time (min) from solubility test.
[b] Fractional conversion at t_g.
[c] Gel time (min) from stirrer test.

during the course of reaction on an arbitrary scale and the results presented diagramatically in Figure 5. With toluene as diluent, the reaction systems stay quite clear until well beyond the gel point, however adjudged. However, a faint turbidity appears at higher conversions, the more readily the greater the content of divinylbenzene isomers. At first crosslinker content, the incidence of phase separation is related to the diluent content; and at a low level of toluene (.322/.231/T), the reaction remains clear to beyond 60% conversion. With this solvating diluent, the appearance of scattering centers must be due to a microsyneresis as the gel formed locally deswells to conform to equilibrium conditions

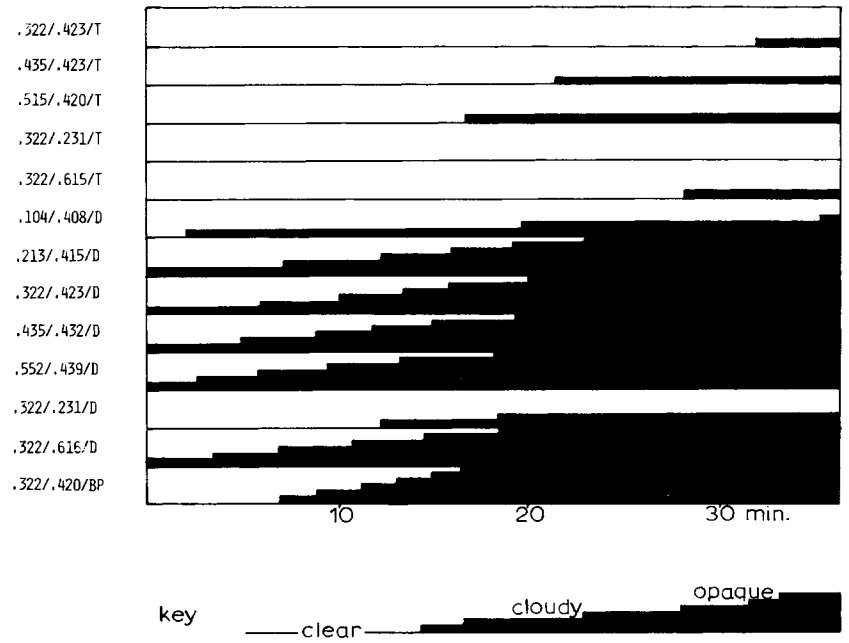

Fig. 5. Phase separation during reaction: diagrammatic representation in terms of visual assessment of turbidity development.

imposed by the balance between osmotic expansion and elastic retraction (Flory–Rehner).[18] None of the reactions showed signs of gross (macro) syneresis even at completion of reaction.

With nonsolvating diluents, phase separation occurs prior to gelation, with one exception only (.322/.231/D).

Having summarized features of the polymerization, it is now necessary to turn to the properties of the network structures so produced. The total porosity of polymer beads was established by measurement of their apparent densities with mercury as confining fluid. Mercury is not able to penetrate pores having entrances less than the critical value given by the Young–Laplace equation. Assuming the pores to be cylinders of circular cross section, the critical radius for mercury at atmospheric pressure is 72600 Å. Thus, if ρ is the matrix density and ρ_a the density in mercury, the pore volume per unit mass (ϕ) for pores less than the critical radius (which we take to be the total porosity) is given by

$$\phi = \left(\frac{1}{\rho_a} - \frac{1}{\rho}\right) \tag{1}$$

A value of $\rho = 1.042$ g/cm^3 is used; this is the mean value found for beads prepared in the absence of diluent and lies within the range (1.040 to 1.065 g/cm^3) quoted in the literature.[19] The values of ϕ are the means from three separate determinations of ρ_a; and, for $\phi > 0.07$, the standard deviations do not exceed 2% of this mean value. Pore volumes for beads made with a diluent volume fraction of 0.42 are plotted in Figure 6 as a function of crosslinker content. If the monomers were converted to solid polymer on polymerization and the volume occupied by diluent becomes the void volume, a limiting pore volume, ϕ_{lim}, may be defined as equal to $V_D/V_M\rho_M$, where V_D is the volume fraction of diluent, V_M is that of monomer, and ρ_M is the monomer density. The limiting value appropriate to the data of Figure 6 is $\phi_{\text{lim}} = 0.76_0$ g/cm^3 and is equal to the plateau

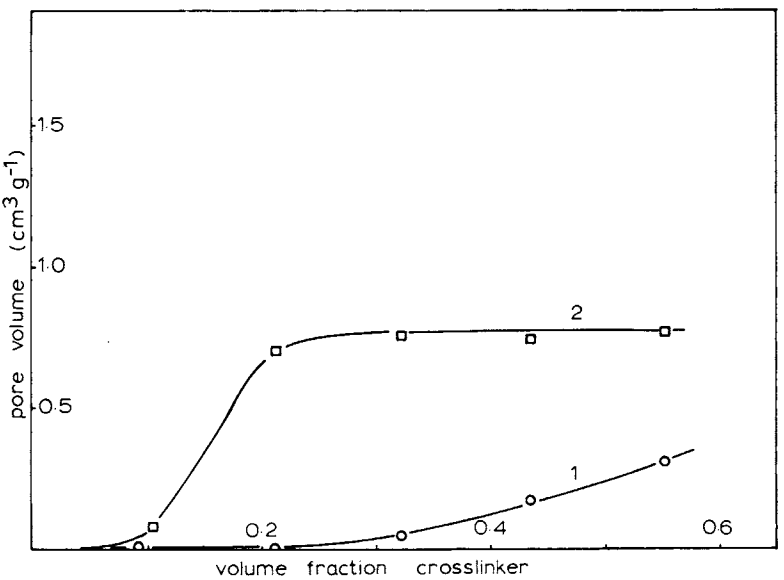

Fig. 6. Pore volume at approximately 0.42 volume fraction diluent as function of divinylbenzene content of monomer: Curve 1, toluene as diluent; Curve 2, decane as diluent.

attained by the decane-modified preparations. The variation in polymer porosity with diluent content at fixed monomer composition is given in Figure 7, where the theoretical ϕ_{lim} curve is also sketched; again, this limit is only approached by nonsolvating diluent at higher contents. The pore volumes produced by the diluents are listed in Table 6.

With the exception of the butyl phthalate sample, the pore volumes of the beads depends on the solvating power of the diluent as expressed by its solubility parameter.

The mercury penetrometer used for pore size distribution studies had an upper pressure limit of 5000 psi, and thus only pores of equivalent radii greater than 210 Å were sensed. The distributions for toluene-modified beads are given in Figure 8. At fixed crosslinker and varying diluent contents, the absolute distributions are rather similar, but at higher toluene contents, the content of larger pores is increased. In all cases, only some 30–40% of the total pores are larger than 210 Å equivalent radius. As the divinylbenzene content is increased, at a fixed volume fraction of toluene there is a decrease in the proportion of pores

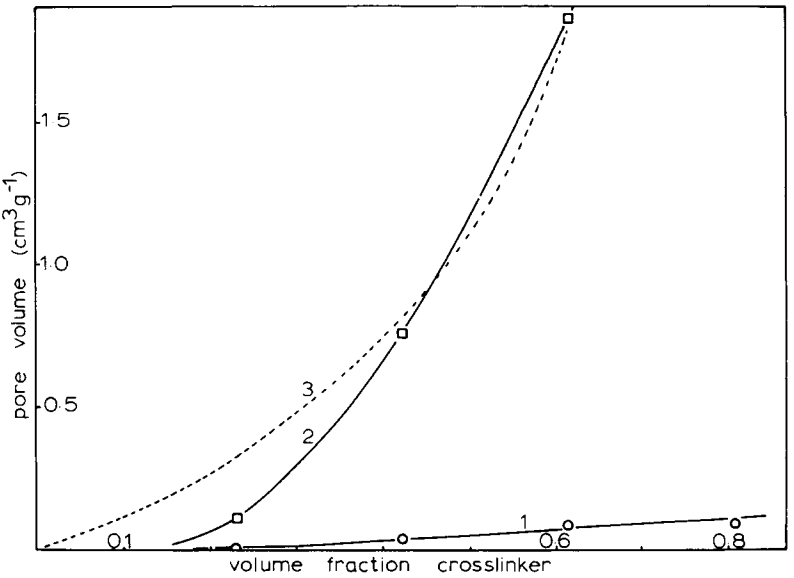

Fig. 7. Pore volume at 0.322 volume fraction divinylbenzene as function of diluent content: Curve 1, toluene; Curve 2, decane; Curve 3, ϕ_{lim}.

TABLE VI
Pore Volume as Function of Nature of Diluent[a]

Diluent	Pore volume, cm^3/g	Solubility parameter of diluent, $cal^{1/2}/cm^{3/2}$
Tetrachloroethane	zero	9.7
Ethylbenzene	$0.0340 \pm 0.005_6$	8.8
Toluene	$0.036_8 \pm 0.000_8$	8.9
Xylene	$0.073_3 \pm 0.001_0$	8.8
Dibutyl phthalate	$0.505_9 \pm 0.003_4$	9.3
Decane	$0.757_1 \pm 0.004_1$	6.6

[a] 0.322 Volume fraction divinylbenzene in monomer, 0.423 volume fraction of diluent.

TABLE VII
Surface Areas from Nitrogen Adsorption

Sample code	Surface area, m^2/g	Mean radius, Å
.092/.385/T	—[a]	—
.213/.415/T	—	—
.322/.423/T	—	—
.435/.432/T	0.8	4270
.552/.439/T	420	14.7
.322/.231/T	—	—
.322/.615/T	—	—
.322/.808/T	—	—
.104/.408/D	6.2	254
.213/.415/D	89.0	158
.322/.423/D	109.0	139
.435/.432/D	161.0	92
.552/.439/D	186.0	82.6
.332/.231/D	8.5	263
.332/.616/D	88.0	422
.322/.423/BP	168.0	63.2

[a] Too small to measure.

> 210 Å, with samples .435/.432/T and .552/.429/T being virtual identical in pore distribution although different in total porosity. Again, most of the total pore volume is in pores too small to be penetrated by mercury at 5000 psi, and the data from this technique are restricted to the high radius tail of the distribution.

Decane-modified samples (Fig. 9) of constant crosslinker content have distributions which are very sensitive to the diluent content, and sample .322/.616/D is seen to be very largely composed of wide pores within the range of the porosi-

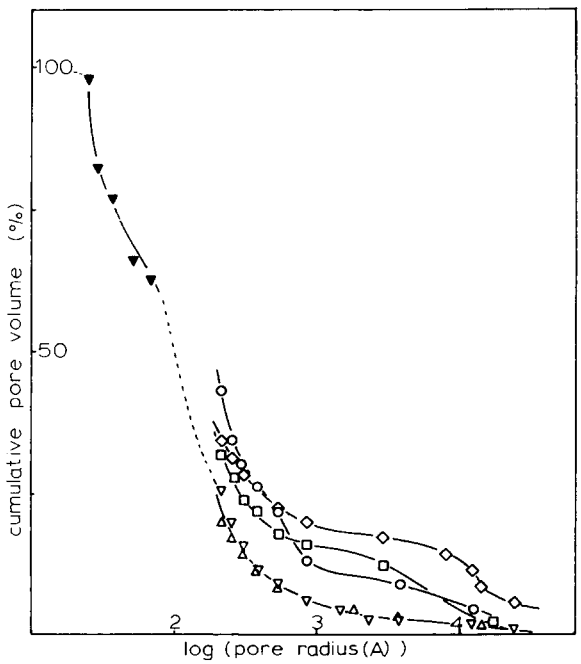

Fig. 8. Pore size distribution of toluene-modified beads: (⊙) .322/.423/T; (⊡) 322/.615/T; (◈) .322/.808/T; (◬) .435/.432/T; (▽) .552/.439/T; filled symbols, by nitrogen desorption.

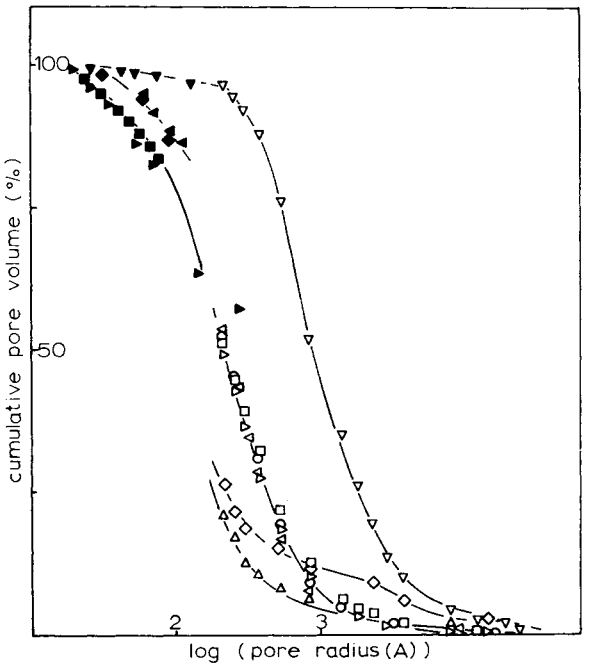

Fig. 9. Pore size distribution of decane-modified beads: (△) .322/.231/D; (○) .322/.423/D; (▽) .322/.616/D; (◇) .104/.408/D; (◁) .213/.415/D; (▷) .435/.432/D; (□) .552/.439/D; filled symbols, by nitrogen desorption.

meter. At a fixed volume fraction of 0.42 decane, the total porosity is approximately constant above 0.2 volume fraction of divinylbenzene (Fig. 6), and the pore size distributions are almost coincident while 0.104/.408/D has a broader pore distribution. Sample .322/.423/BP, which is of quite high porosity, has few larger pores, only 10% of the pore volume being accommodated in pores greater than 500 Å equivalent radius. The low-porosity sample .322/.423/EB has a distribution curve similar to toluene-containing preparations of the same diluent volume fraction but higher crosslinker.

Adsorption of nitrogen gas at −196°C is a well-known method of characterizing porous solids. In the present report, apparent surface areas are estimated from the BET analysis of the isotherm (Table VII); full sorption–desorption isotherms were determined on selected samples in order that the Kelvin analysis of the desorption branch could be used to find the pore size distribution. The isotherm shown (Fig. 10) is of one of the more porous specimens; the good repeatability of the two separate experiments is evident, as is the extensive hysteresis on desorption. The lengthy equilibration period required for each datum point limited the acquisition of desorption data. Two further features are noticeable in Figure 10. The isotherm shows no indication of leveling-off at high relative pressures, which implies a continuous distribution of pores into the macropore region. Further, the initial portion of the isotherm shows a substantial adsorption at very low relative pressure, which might be a consequence of micropores.

Low-porosity samples have very small surface areas which cannot be measured to any accuracy; zero-diluent samples had no detectable surface area by nitrogen adsorption. Only one sample from the series made with toluene as diluent is of high surface area; this is the sample of highest divinylbenzene content. The

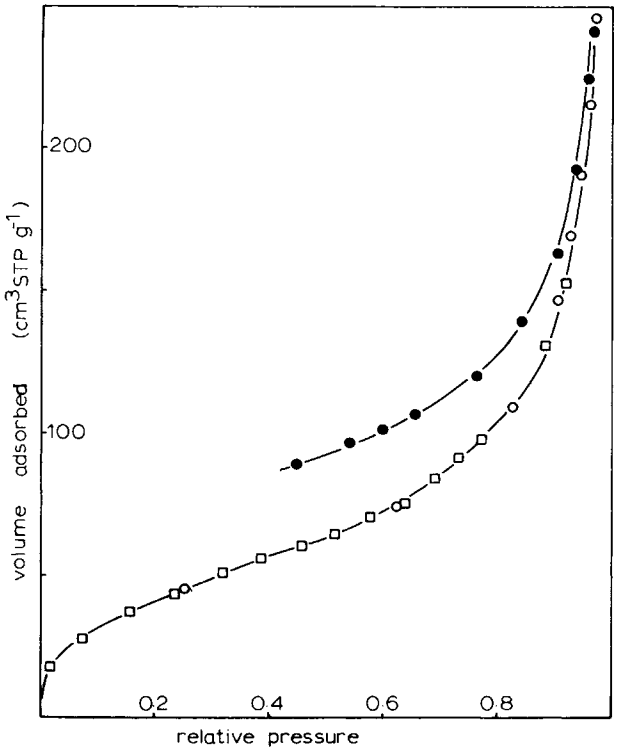

Fig. 10. Nitrogen sorption isotherm of .435/.432/D (two experiments); filled symbols, desorption.

other toluene-modified bead polymers adsorb very little nitrogen even at relative pressures around 0.9, which implies an absence of pores below 100 Å equivalent radius. Decane-modified samples show increasing surface areas with increasing crosslinker content, even where the total porosity is constant. The effect of diluent content at fixed crosslinker is less clear, except that a certain level is necessary for substantial internal area. The lower surface area of .332/.616/D is a consequence of the larger average pore dimensions of this very highly porous sample.

Table VIII allocates the proportion of the total pore volume detected by ni-

TABLE VIII
Proportion of Total Pore Volume Detected by Mercury Intrusion and by Nitrogen Sorption

Sample code	% Pore volume by mercury intrusion	% Pore volume by nitrogen sorption	Equivalent pore radius at maximum p/p_0, Å
.322/.423/T	43.2	3.0	158
.104/.408/D	26.7	56.0	200
.213/.415/D	53.4	28.9	163
.322/.423/D	52.6	12.4	58
.435/.432/D	49.3	51.4	300
.552/.439/D	51.2	45.2	108
.332/.231/D	21.4	16.1	400
.332/.616/D	96.5	5.5	180

trogen sorption and mercury intrusion, respectively. With one exception (.322/.231/D), the separate assessments are reasonably consistent when allowance is made for the gap between the upper limit of the gas adsorption data and the lower bound of mercury porosimetry, which is in some cases a wide one.

An apparent mean pore radius may be deduced by comparison of the BET surface area with the total pore volume, and these values have been included in Table VII. However, in most cases, the values do not seem in accord with the pore size distributions of Figures 8 and 9; both analysis rely on a uniform cylindrical pore volume. The apparent discrepancy may be taken to cast doubt on the significance of some of the BET surface areas. In many porous solids, high apparent surface areas are often a consequence of condensation in micropores at very low relative pressures. A useful test for microporosity is to plot the adsorption data in the form of the Dubinin equation.[20] When this is done, however, the fit to a single linear plot is poor, and the recorded values (Table IX) must be regarded as highly approximate. Also recorded in this table are the volumes of micropores that would be equivalent to the meaured BET surface area: the shape of the isotherms is such that this latter assumption must be a considerable overestimate. Nonetheless, the apparent micropore volumes from the Dubinin equation are consistently even higher, and so this interpretation must be rejected. Sample .552/.439/T is somewhat anomalous in that its high surface area predicts a much lower mean pore dimension than is consistent with the distribution curve of Figure 8 and may be that some of this apparent surface area is to be attributed to a process of micropore filling although perhaps not to the extent implied by the results of Table IX. The nitrogen adsorption isotherm of this sample has a sharp "knee," 42% of the total nitrogen sorption being reached by a relative pressure of 0.10.

The desorption behavior of six samples was analyzed by the pore-emptying hypothesis,[9] and the resultant pore size distributions are included in Figures 8 and 9. Despite the generally satisfactory concordance of the nitrogen data at the small pore region of the distribution with the mercury porosimeter results in the macropore range, there is nevertheless some doubt on the validity of the gas desorption analysis. The desorption isotherm from a porous rigid solid would be expected to close at relative pressures around 0.4. However, in all those samples in which desorption was continued to low relative pressures, no closure of the hysteresis loop was detected. Hoburg et al.[21] have reported low-pressure hysteresis of nitrogen in linear polystyrene which they attribute to penetration

TABLE IX
Apparent Microscope Volumes from Nitrogen Sorption

Sample code	Micropore volume by Dubinin equation		Micropore volume equivalent to BET surface area	
	cm^3/g	% of total	cm^3/g	% of total
.552/.439/T	0.183	59.4	0.150	48.7
.104/.408/D	0.004	5.1	0.002	2.5
.213/.415/D	0.054	7.7	0.031	4.4
.322/.423/D	0.047	6.2	0.039	5.2
.435/.432/D	0.087	11.7	0.057	7.7
.552/.439/D	0.064	8.3	0.066	8.6
.322/.616/D	0.044	2.4	0.031	1.7

of the absorbate into the molecular structure of the polymer. It may be, however, that on sorption of nitrogen to high relative pressures, the polymer structure opens somewhat, only to collapse on reducing the relative pressure to a morphology with channels of a size such that activated diffusion processes become operative.

One of the highly porous samples (0.322/.616/D) was partially ground and its BET surface area redetermined. A progressive drop in the initial region of the nitrogen isotherm occurs, with a consequent lowering of the BET area: whereas the original sample had an area of 88 m^2/g, a part-ground one gave 80 m^2/g while the fully ground sample dropped to 70 m^2/g. These results suggest that mechanical damage removes some of the structural features responsible for the relatively large adsorption at low relative pressure.

Vapor sorptions were also measured, by the gravimetric technique, both with an adsorbate thought to be nonswelling and one known to swell the matrix polymer. Methanol absorbs at 30°C to give a type III isotherm (Fig. 11); and with the sample shown, the desorption hysteresis persists to low relative pressures. The volume of methanol adsorbed close to saturated vapor pressure (actually at $p/p_0 = 0.985$) is compared in Table X to the total pore volume deduced from the densities in mercury. It would seem that methanol is taken up to some extent into the molecular structure of the polymer and that it is not entirely nonswelling to polystyrene/divinylbenzene. The type III isotherm is of the same shape as that required by an equilibrium swelling mechanism of the Flory–Rehner type.[18] Whether low relative pressure data could, alternatively,

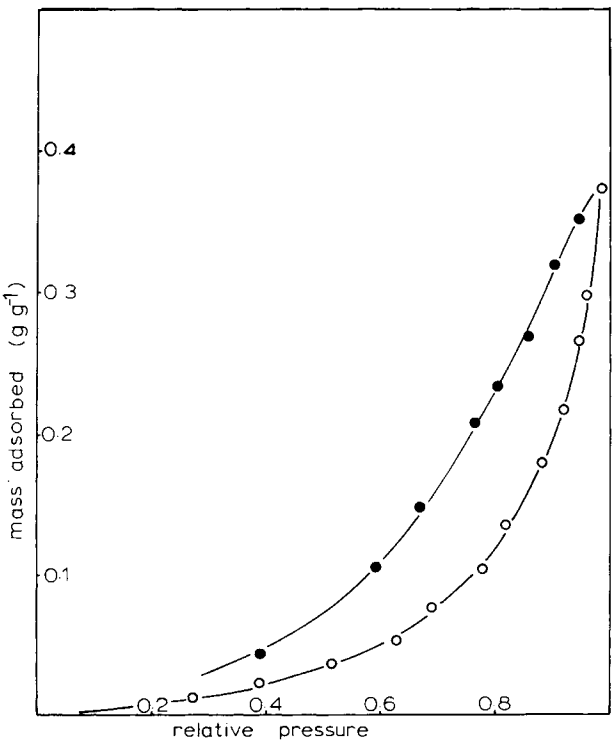

Fig. 11. Methanol sorption isotherm of .364/.410/T; filled symbols, desorption.

TABLE X
Volume of Methanol Sorbed at $p/p_0 = 0.985$, Compared to Total Pore Volume

Sample code	Volume methanol sorbed, cm^3/g	Pore volume, cm^3/g
.364/.410/T	0.48	0.08
.515/.420/T	0.65	0.28
.600/.430/T	0.70	0.34
.515/.250/D	0.35	0.37
.515/.420/BP	0.71	0.60

be interpreted as a physical sorption on a solid surface is not easily deduced, especially as the BET analysis cannot be used for surface area estimation with type III isotherms. According to Gregg and Sing,[9] when the c constant of the BET equation takes values of between 1 and 5, which are characteristic of type III isotherms, the adsorption that is equivalent to the monolayer capacity occurs at relative pressures between 0.3 and 0.5. On this basis, the samples of Table X would have surface areas within the range 40–280 m^2/g, which would not be inconsistent with the values expected, by analogy with other samples (Table VII), from nitrogen adsorption.

Toluene would be the natural selection as a swelling sorbate; however, benzene was substituted for the experimental convenience of its higher vapor pressure at the working temperature. For one sample at least, the two vapors yield similar isotherms on a mass basis (Fig. 12), and we believe that the sorption behavior

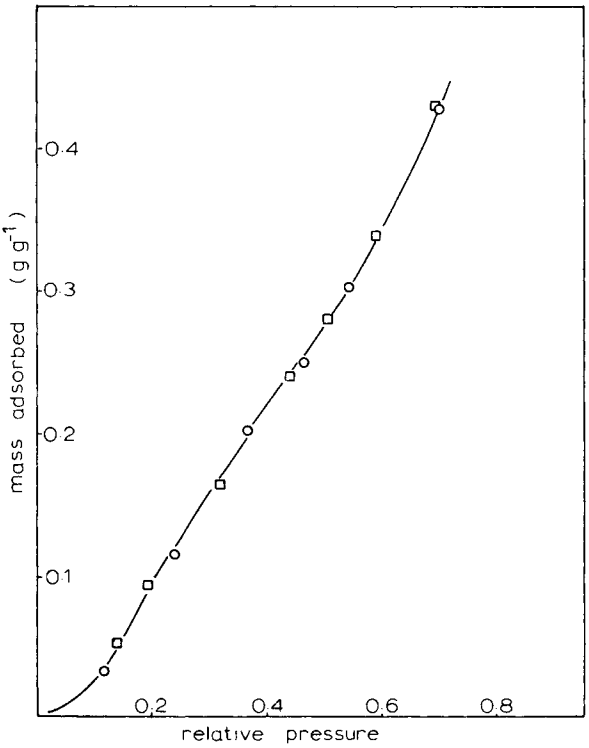

Fig. 12. Vapor sorption isotherms of .364/.410/T: (⊙) toluene; (⊡) benzene.

of these two vapors will be very similar with all the polymer samples. The benzene isotherms are of type II with the more porous beads and with all other samples are more like Figure 12 in that the initial portion is type III but with an increment in sorption at higher relative pressures. In no case is a simple swelling curve, with monotonically increasing slope, observed. Equilibrium sorption can be very slow, up to several days, the rate increasing with increasing relative pressure and crosslinker and diluent contents. Polymer beads made without diluent at lower crosslinker levels (0.1–0.2 volume fraction) are so slow in vapor sorption that isotherms could not be measured. Only a limited amount of desorption studies were attempted, but desorption hysteresis was generally observed except in the case of the very porous sample .322/.616/D. The apparent pore volumes as given by the volume of benzene adsorbed at $p/p_0 = 0.985$ are given in Table XI. Except for the highly porous sample (.322/.616/D), the benzene values are in excess of the physical pore volume. Furthermore, more benzene is taken up than is methanol, as would be expected on general solubility grounds.

At a fixed level of divinylbenzene, the amount of benzene vapor adsorbed by the polymer increases with the solvating diluent content present during polymerization but is relatively independent of the crosslinker content at a constant diluent level. The latter is not what would be expected from the swelling of a homogeneous network. The same trends seem to hold also for the decane-modified samples, which have higher adsorptions than the corresponding toluene-modified beads. Again, if benzene uptake from the vapor phase were a simple gel swelling of a uniform network, no difference between the two series would be expected.

The general features of the benzene vapor sorption isotherms are of a physical adsorption at low relative pressures followed by a penetration of the structure to open up new sites at moderate relative pressure. At rather higher relative pressures, a general sorption/swelling process develops. Initial adsorption at low relative pressures may, with the more highly crosslinked samples, be comparatively high and greater than the adsorption of samples which, at high relative pressures, sorb more benzene. This complexity is probably a consequence of the higher physical adsorption at low p/p_0 on the larger surfaces of the more inhomogeneous samples, which are too highly crosslinked to show much swelling at high relative pressures.

TABLE XI
Volume of Benzene Sorbed at $p/p_0 = 0.985$, Compared to Total Pore Volume

Sample code	Volume benzene sorbed, cm^3/g	Pore volume cm^3/g	Sample code	Volume benzene sorbed, cm^3/g	Pore volume cm^3/g
.322/.231/T	0.41	0.008	.322/.213/D	0.52	0.112
.322/.423/T	0.86	0.037	.322/.423/D	n.d.	0.757
.322/.615/T	1.57	0.080	.322/.616/D	1.00	1.86
.322/.808/T	1.86	0.087	.104/.408/D	1.45	0.079
.092/.385/T	0.86	0.011	.213/.415/D	1.22	0.702
.213/.415/T	0.74	0.001	.435/.432/D	1.08	0.741
.435/.432/T	0.89	0.171	.552/.439/D	1.01	0.769
.555/.439/T	0.84	0.308	.322/.037	0.33	zero
.322/.432/EB	0.75	0.034	.435/.051	0.17	zero
			.552/.063	0.17	zero

The equilibrium swelling in liquid toluene was also measured both by the centrifuge technique[11] and microscopically[12] on individual beads. However, the latter method introduced some uncertainties and in some cases gave lower results than the centrifuge technique (Table XII). The present discussion is, therefore, restricted to swelling data obtained by Pepper's method.[11]

The amount of toluene sorbed from the liquid phase is generally greater than the amount of benzene vapor taken up at high relative pressures, especially in the case of the more porous samples where the difference must largely represent the volume of the larger pores which remain unfilled in sorption from the vapor phase (Table XIII). The equilibrium swelling of nonporous samples, i.e., those polymerized in the absence of diluent, should obey an equation of the form of the Flory–Rehner equation.[18] A complete agreement cannot be expected for such highly crosslinked and highly entangled networks. Nonetheless, apparent values of an effective molecular weight between crosslinks (M_e) have been calculated from the Flory–Rehner equation from the toluene swelling data, using a value of 0.44 for the interaction parameter (χ). These values (final two columns of Table XIV) cannot have any absolute significance, and indeed, some fall below the limit of 130 for a perfect divinylbenzene network. For the nonporous samples, the M_e values are practically linear with the reciprocal of the divinylbenzene

TABLE XII
Comparison of Observed Swelling Ratios with Values Calculated from Swelling Data from the Centrifuge Technique

Sample code	Observed swelling ratio	Calculated swelling ratio	Sample code	Observed swelling ratio	Calculated swelling ratio
.322/.231/T	1.3_2	1.6_2	.322/.213/D	1.3_9	1.4_6
.322/.423/T	1.7_5	2.0_1	.322/.423/D	1.1_9	1.1_7
.322/.615/T	2.5_4	2.8_1	.104/.408/D	2.0_4 (2.4_2)[a]	2.3_0
.092/.385/T	2.1_6	2.4_2	.213/.415/D	1.2_9	1.2_4
.213/.415/T	1.9_6	2.1_3	.435/.432/D	1.0_9	1.1_0
.435/.432/T	1.6_4	1.6_4	.552/.439/D	1.0_6	1.0_8
.435/.051	1.1_2	1.2_3	.552/.063	1.1_2	1.1_8

[a] Value in parentheses for translucent beads.

TABLE XIII
Comparison of Swelling in Benzene Vapor (at $p/p_0 = 0.985$) and in Liquid Toluene

Sample code	Uptake of benzene vapor, g/g	Uptake of toluene, g/g	Sample code	Uptake of benzene vapor, g/g	Uptake of toluene, g/g	Sample code	Uptake of benzene vapor, g/g	Uptake of toluene, g/g
.322/.231/T	0.36	0.52	.322/.213/D	0.45	0.52	.322/.037	0.28	0.26
.322/.423/T	0.74	0.91	.322/.423/D	n.d.	0.92			
.322/.615/T	1.35	1.70	.322/.615/D	0.86	1.80			
.322/.808/T	1.60	4.15						
.092/.385/T	0.74	1.20	.104/.408/D	1.25	1.23	.104/.012	n.d.	0.59
.213/.415/T	0.64	0.94	.213/.415/D	1.05	0.95	.213/.025	n.d.	0.36
.435/.432/T	0.77	0.78	.435/.432/D	0.93	0.79	.435/.051	0.15	0.19
.555/.439/T	0.73	0.72	.552/.439/D	0.87	0.78	.552/.063	0.15	0.15

TABLE XIV
Effective Molecular Weight Between Crosslinks (M_e) (Flory–Rehner[18] Equation)

Sample code	M_e	Sample code	M_e	Sample code	M_e
.322/.231/T	171	.322/.213/D	134	.322/.037	81
.322/.423/T	397	.322/.423/D	83		
.322/.615/T	1024	.322/.615/D	66		
.322/.808/T	5280				
.092/.385/T	710	.104/.408/D	568	.104/.012	210
.213/.415/T	368	.213/.415/D	109	.213/.025	114
.435/.432/T	226	.435/.432/D	50	.435/.051	61
.555/.439/T	168	.552/.439/D	42	.552/.063	50

content. Furthermore, the toluene swellings of these samples agree closely with the data of Pepper[11] (Fig. 13).

When the polymers are porous, the swelling is a composite of the filling of the pores and the matrix swelling. The values of Table XIV for porous samples are calculated on the following basis. The volume of toluene filling the pores is taken to be the same as the pore volume from the densities measured in mercury; this is subtracted from the observed swelling, and the resultant is used to calculate M_e. At a constant divinylbenzene content, the effective crosslink density is very dependent on the amount of solvating diluent present during polymerization; and, at 0.80 volume fraction, M_e rises to approximately 5000. This effect is due to the enhanced intramolecular reactions, which form elastically "wasted" links in the presence of diluent, and is a well-known phenomenon in homogeneous gelation.[22,23] At fixed diluent level, the values of M_e are much less dependent on divinylbenzene content. When the diluent is nonsolvating, the greater part of the crosslinking reaction takes place in a precipitated, although swollen, phase. Thus, the results at fixed divinylbenzene concentration but varying diluent do

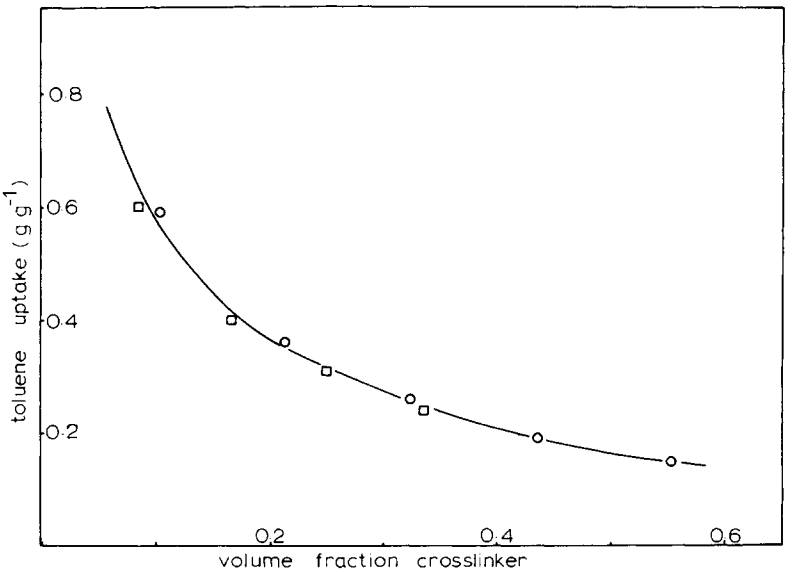

Fig. 13. Swelling in toluene of nonporous polymers as function crosslinker content: (⊙) present work; (⊡) data of Pepper.[11]

not show the "wastage" effect observed with a solvating diluent; correspondingly, at fixed diluent, the dependence of M_e on divinylbenzene content remains large.

Millar et al.[4] have shown the usefulness of the simple equation

$$U = U_0 + D \tag{2}$$

where U is the equilibrium volume of swelling liquid per unit mass of dry polymer, U_0 is the corresponding value for an otherwise equivalent polymer made without diluent, and D is the volume of diluent per unit mass of monomer during bead formation. The data obtained at constant crosslinker content (volume fraction 0.322) fit a similar equation:

$$U = U_0 + kD \tag{3}$$

with $k = 0.97$ (Fig. 14).

Transmission electron microscopy was made on microtomed slices approximately 600 Å thick. Figure 15(*a*) shows the internal structure of a polymer sample of moderate porosity (.555/.439/T, $\phi = 0.308$) made with a solvating diluent. The basic structure is one of fine grains of polymer fused together, but with some larger voids ($>10^3$ Å). The more porous samples made with nonsolvating diluent tend to fracture on being cut. Figure 15(*b*) shows that the basic globules are much larger, but it is not certain whether some of the large voids are part of the structure or have been formed on slicing the specimen. A diluent of intermediate solvating power, butyl phthalate, gives an intermediate structure [Fig. 15(*c*)] with granules approximately 500–1000 Å in diameter. Samples made without diluent, or with low levels of toluene, are found to be featureless on examination by transmission electron microscopy.

Scanning electron microscopy, by virtue of its greater depth of field, shows more clearly the microglobular nature of the internal structure. Figure 16(*a*)

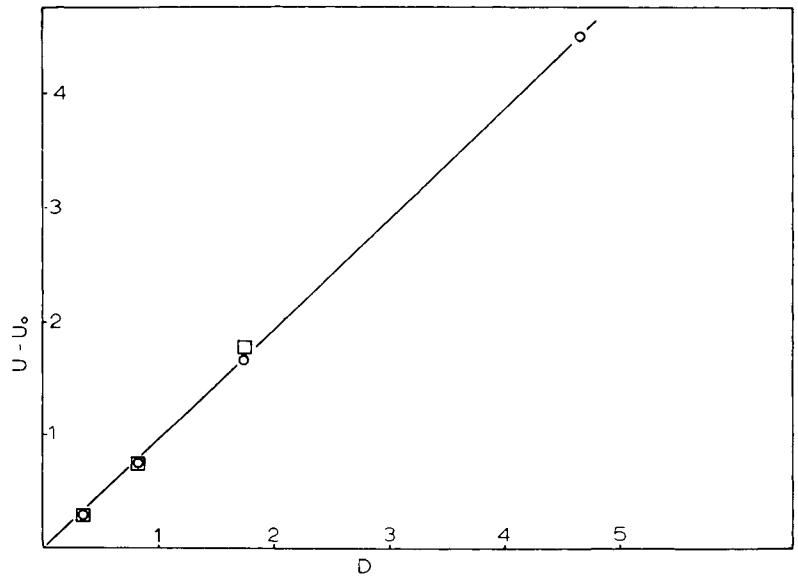

Fig. 14. Plot of eq. (3): (⊙) toluene-modified beads: (⊡) decane-modified beads.

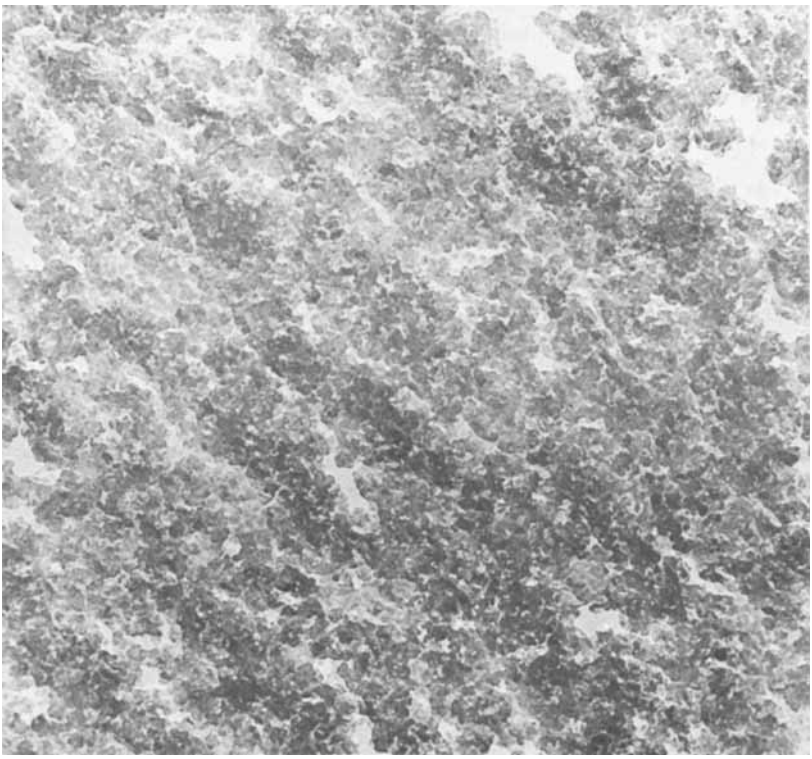

(a)

Fig. 15. Transmission electron microscopy: (*a*) .555/.439T ×73500; (*b*) .322/.423/D ×71400; (*c*) .322/.423/BP ×18900.

shows the interior of the very porous sample (.322/.615/D); the external surface [Fig. 16(*b*)] is less porous, with indications of a skin as found with some other suspension-polymerized polymers.[3] If the surface area is that of the fused microglobules that constitute the bead interior, values ranging from 10 to 300 m^2/g would result from microglobule diameters in the observed range of 6000 to 200 Å.

DISCUSSION

Porosity in the suspension-polymerized styrene–divinylbenzene copolymers is always induced by nonsolvating diluent, whereas those samples made without diluent are nonporous. Solvating diluents occupy an intermediate position in that nonporous beads are produced at lower crosslinker and diluent contents but, at the other extreme, some porosity is produced. Although the working-up state involves the deswelling of suspension-polymerized polymer made with solvating diluents, we believe that most, if not all, the properties of the final beads are fixed by events during the copolymerization. This copolymerization is a complex one: in the first place, it is really a quaternary copolymerization in that the commercial divinylbenzene contains ethylstyrene and two divinylbenzene isomers.

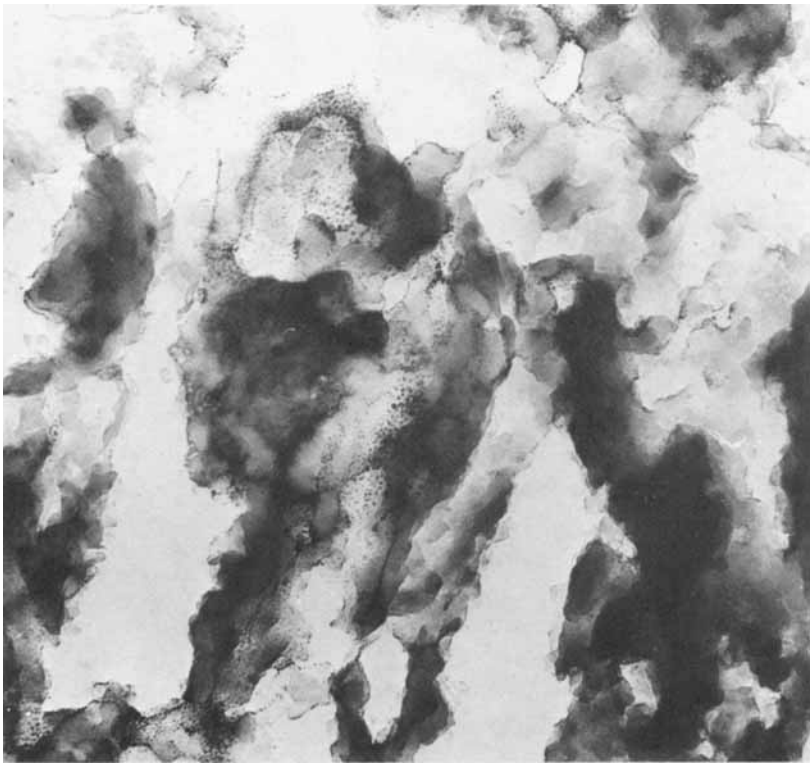

(b)

Fig. 15 (*Continued from previous page.*)

The higher reactivity of the divinylbenzene, especially of the paraisomer, means that the initially formed polymer will be preferentially rich in the tetrafunctional comonomer. The implications of the varying polymer composition with conversion have been discussed by Schwachula.[24] The net solvating power of the medium also changes during the course of reaction as the monomers become consumed, and this alteration will be particularly severe where the diluent is nonsolvating for the polymer. The various diluents may have one further effect—that of chain transfer, which would increase the number of dangling ends in the network and so reduce its elastically effective crosslink density. In the present case, chain transfer cannot be very significant to judge by the data of Table XV, which records the effect of analogous amounts of the diluents in styrene homopolymerization. Under the experimental conditions chosen for bead polymerization, especially the relatively low initiator content, chain transfer effects are likely to be very small.

The formation of inhomogeneities during polymerization with nonsolvating diluent is clearly a case of what is described by Dusek[26] as χ-induced syneresis. The unfavorable medium leads to polymer precipitation very early in reaction and prior to the gel point. This early precipitated polymer will be rich in trapped, unreacted vinyl groups and will be the nucleus of the microglobules seen in the electron micrographs. These nuclei are regions of relatively high crosslink density, but the final beads will have a graduation of crosslinking through the

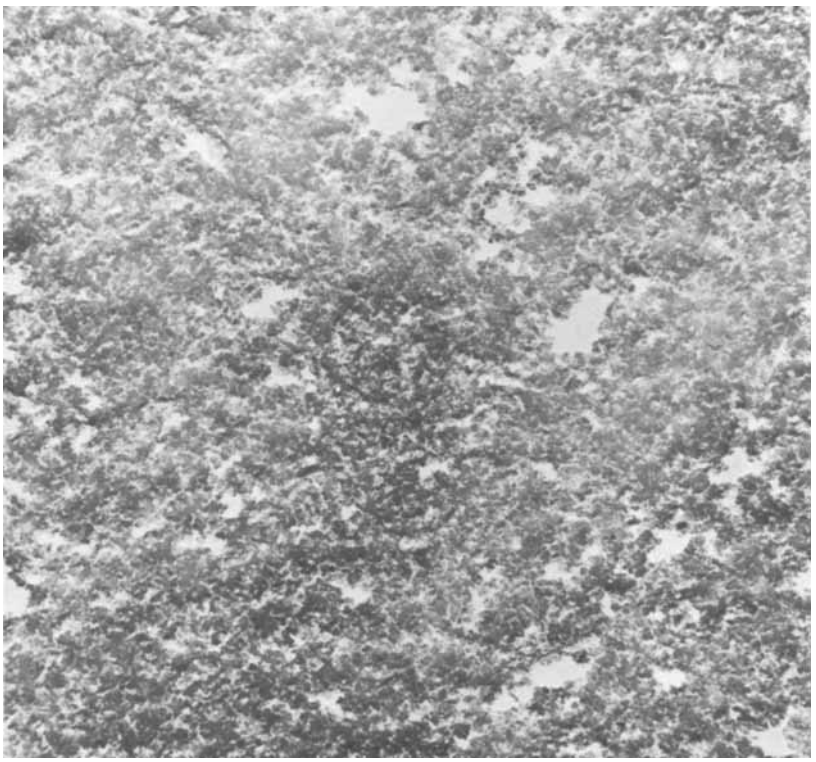

(c)

Fig. 15 (*Continued from previous page.*)

microglobules. Differential wetting may cause some of the first-formed polymer to congregate near the interface. Electron microscopy suggests the surface to be less macroporous than the interior, and one preparation, at least, is altered in its sorption properties by mechanical break-up of the bead structure.

When the decane content is high, the precipitated phase will be largely unswollen so that the microglobules will be "solid" polymer similar to the whole beads made without diluent. As a consequence, the final void volume should closely approach the volume of nonsolvating diluent, as is found.

At low decane contents, the early precipitated phase will be relatively swollen, and gradual syneresis during reaction will ensure that the final void volume is less than that of the diluent. No gross macrosyneresis was observed, in the sense of an upper liquid layer, in the tube experiments even after 24 h of reaction with a nonsolvating diluent. When both the divinylbenzene and decane contents are low, the working-up procedure may allow swelling and consequent collapse so that the dried polymer beads may have lower than expected porosity (Fig. 7).

With a solvating diluent, gelation occurs before the appearance of visible phase separation, although such phase separation will be difficult to detect where the precipitated polymer is highly swollen by a liquid of similar refractive index. It does not necessarily follow that a macroscopically homogeneous network is formed, and the lack of concordance between the different ways of judging the gel point may indicate that, even in toluene, discrete regions of gel are first

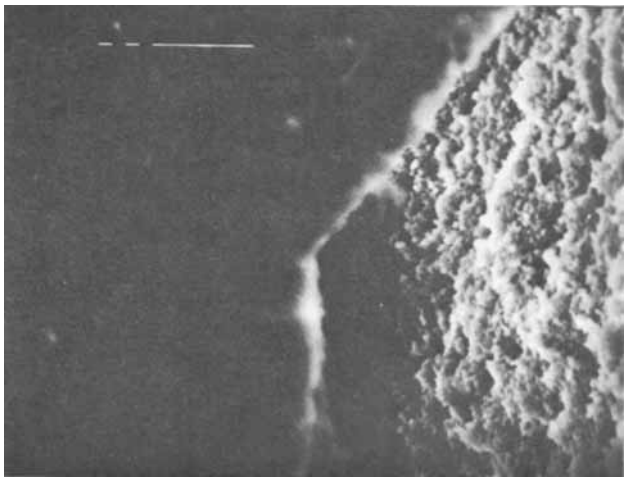

(a)

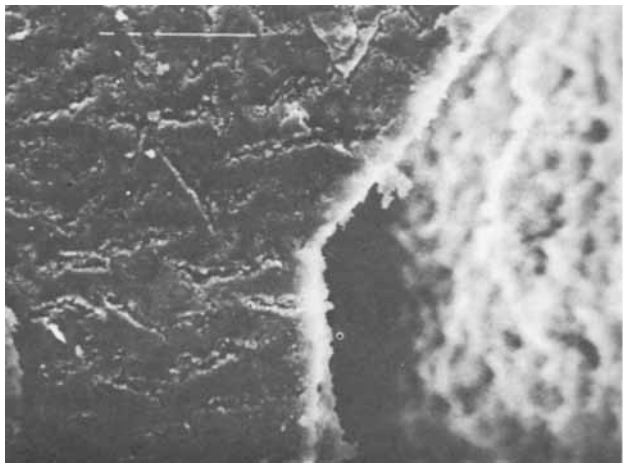

(b)

Fig. 16. Scanning electron microscopy: (*a*) .322/.615/D ×2000, interior structure in focus; (*b*) as (*a*), external surface in focus.

formed. Nonetheless, when the crosslinker and diluent concentrations are low, the network is able to fill the whole volume available. On subsequent treatment, the beads deswell sufficiently uniformly to prevent the development of more than trivial amounts of porosity. However, as the divinylbenzene content (or, to a lesser extent, the toluene content) is increased, a point is reached during the reaction in which the crosslink density in the forming network is too high for it to accupy the total volume of the reaction system. This is the phenomenon Dusek[26] calls ν-induced syneresis. Although kinetic factors must be important in the process, the observation of visual turbidity during polymerization with solvating diluents in those cases that lead to porous polymers implies a microsyneresis. That is, in regions where the crosslink density is locally high, deswelling sets in and the resulting heterogeneities are the nuclei of the microglobules seen in the electron micrographs [e.g., Fig. 15(a)].

TABLE XV
Degree of Polymerization of Polystyrene Made in Presence of Diluents (Conditions as in Styrene–Divinylbenzene Copolymerization)

Diluent	Volume fraction	$\bar{x}_v$[a]
Toluene	0.05	8880
Toluene	0.10	8390
Toluene	0.15	8300
Toluene	0.20	8020
Decane	0.05	8490
Decane	0.10	8300
Decane	0.15	8200
Decane	0.20	7730
Ethylbenzene	0.10	7880
Dibutyl phthalate	0.10	8200
Xylene	0.10	7730
Tetrachloethane	0.10	7370
No diluent	—	9450

[a] From intrinsic viscosity in benzene and equation of Orofino and Wegner.[25]

One of the authors (C.A.M.) is indebted to the Science Research Council for the award of a Research Studentship during the tenure of which (1966–69) this work was carried out.

References

1. K. A. Kun and R. Kunin, *J. Polym. Sci.*, **C16,** 1457 (1967).
2. J. C. Moore, *J. Polym. Sci.*, **A2,** 835 (1964).
3. G. J. Howard and S. Knutton, *J. Appl. Polym. Sci.*, **19,** 697 (1975).
4. J. R. Millar, D. G. Smith, W. E. Marr, and T. R. E. Kressman, *J. Chem. Soc.*, 218 (1963).
5. H. L. Ritter and L. C. Drake, *Ind. Eng. Chem. (Anal. Ed)*, **17**(12), 782, 787 (1945).
6. V. T. Crowl, *Proc. Conf. Particle Size Analysis*, Society for Analytical Chemistry, 1967, p. 288.
7. British Standard 4359, Methods for the Determination of the Specific Surface of Powders, 1969.
8. S. Brunauer, P. H. Emmett, and E. Teller, *J. Am. Chem. Soc.*, **60,** 309 (1938).
9. S. J. Gregg and K. S. W. Sing, *Adsorption, Surface Area and Porosity*, Academic, New York, 1967.
10. J. W. McBain and A. M. Bakr, *J. Am. Chem. Soc.*, **48,** 690 (1926).
11. K. W. Pepper, *J. Appl. Chem.*, **1,** 124 (1951).
12. S. Hudecek and Z. Pelzbauer, *Coll. Czech. Chem. Comm.*, **34,** 349 (1969).
13. J. R. Millar, D. G. Smith, and T. R. E. Kressman, *J. Chem. Soc.*, 304 (1965).
14. M. S. Matheson, E. E. Auer, E. B. Bevilaqua, and E. J. Hart, *J. Am. Chem. Soc.*, **73,** 1700 (1951).
15. P. E. M. Allen and C. R. Patrick, *Makromol. Chem.*, **47,** 154 (1961).
16. E. G. Bobalek, E. R. Moore, S. S. Levy, and C. C. Lee, *J. Appl. Polym. Sci.*, **8,** 626 (1964).
17. B. T. Storey, *J. Polym. Sci.*, **A3,** 265 (1965).
18. P. J. Flory and J. Rehner, *J. Chem. Phys.*, **11,** 521 (1943).
19. E. Brandup and E. Immergut, Eds., *Polymer Handbook*, 1st ed., Wiley–Interscience, New York, 1966.
20. M. M. Dubinin, E. D. Zaverina, and L. V. Radushkevich, *Zh. Fiz. Khim.*, **21,** 1351 (1947).
21. R. F. Hoburg, G. S. Handler, and J. J. Scholz, *J. Coll. Interface Sci.*, **27,** 642 (1968).
22. P. J. Flory, *Principles of Polymer Chemistry*, Cornell University Press, Ithaca, 1953.
23. R. F. Bates and G. J. Howard, *J. Polym. Sci.*, **C16,** 921 (1967).
24. G. Schwachula, *J. Polym. Sci.*, **C53,** 107 (1975).
25. T. A. Orofino and F. Wegner, *J. Phys. Chem.*, **67,** 566 (1963).
26. K. Dusek, in *Polymer Networks; Structural and Mechanical Properties*, A. J. Chompff, Ed., Plenum, New York, 1971, p. 245.

Received March 6, 1981
Accepted April 27, 1981